Dynamic analysis of a 155 mm cannon breech

G. Peter O'Hara
Elmhurst Research, 60 Loudonville Rd., Albany, NY 12204-1513, USA

This report describes a finite element analysis of the breech closure for the 155 mm Cannon M199, which is normally mounted on the Towed Howitzer M198. In this configuration it has has an excellent record for reliability in the field and is easy to service. However when the breech is used in an ammunition test environment, some maintenance problems exist. The analysis is for a 9 body problem with 13 contact surfaces and was solved for both static and dynamic load cases. The two dynamic loads were of similar shape with different loading times. The 9 bodies in the model include, a facility mount, four major structural components, the obturator seal and 3 minor components. The results show that the major components are normally subjected to quasi-static loading but under fast 'pressure spike' loadings, the dynamic effect can be important. This is particularly true for the contact between minor components which can show extreme behavior with the fast loading rates.

1. Introduction

The 155 mm Towed Howitzer M198 has been in service with the US Armed Services since 1978 and has proven to be a reliable weapon with few problems in service. This system uses the 155 mm Cannon M199 which was designed at the Benét Laboratories, with an Eastman style interrupted screw block breech, and a Debange obturator seal. Interrupted screw threads used for the breech block to breech ring connection are also used for the breech ring to barrel connection and in the breech ring to recoil mount joint. A similar interrupted lug joint is used to assemble the firing mechanism housing to the obturator spindle, as a means of allowing easy assembly in the field. While the normal maintenance record of the gun is excellent, there have been some problems with the breech when it is used on ballistic guns for ammunition testing. In this environment the breech is subjected to prototype propellant systems and other conditions which may produce 'ragged' pressure time histories. These histories are characterized by large pressure spikes which apparently do not affect the primary structure but do produce failure in the small components such as the firing mechanism housing. The case in point was the lugs on the obturator spindle which retain the housing on the spindle. These lugs were noted to produce bearing failures which made the components difficult to disasemble. This analysis was intended to explore this effect and demonstrate the value of the analysis of a full cannon breech.

This report will describe the static and dynamic finite element analysis of the breech closure of the M199 cannon. The work compares three different time frames: a static case and dynamic cases using a normal pressure time curve and a very fast pressure spike. The analysis is done at a medium level of detail with the components described by 8 node axisymmetric elements and the various contact surfaces modeled using an appropriate interface formulation. The three major threaded connections are modeled with the individual threads smeared to an equivalent orthotropic continuum and contact modeled using the appropriate kinematics conditions. Other contact surfaces are modeled using either a small sliding or large sliding formulation. All of the necessary analysis tools were available in the ABAQUS Standard finite element code [1,2].

2. Description of component models

The initial objective of this study was to produce individual models of all necessary structural components of the cannon breech and link them to produce the overall system model. This was done with 8 node axisymmetric elements (CAX8) which is a reasonable assumption for these components. The breech ring and block both have non symmetric features but they can be ignored in favor of the more general solution goals. The block carrier is a totally non symmetric structure but this has been ignored because it does not play a structural role during firing. The firing mechanism is another non-symmetric structure, but this level of detail is not appropriate to this analysis. However, it was necessary to include the mass of the firing mechanism in the model of the firing housing.

A cross section drawing of the breech is shown in Fig. 1 with the major components labeled and a brief

Shock and Vibration 8 (2001) 215–221
ISSN 1070-9622 / $8.00

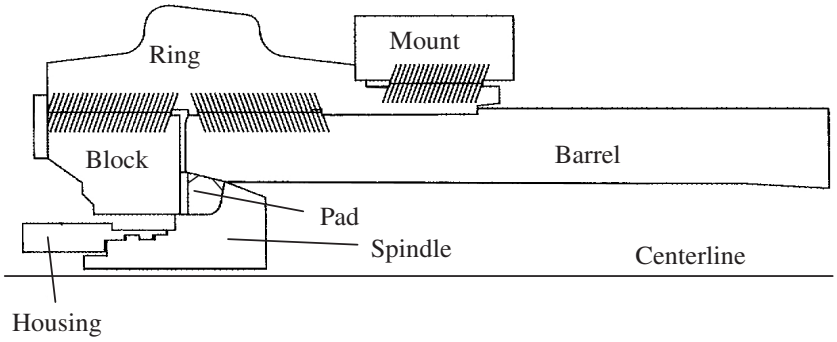

Fig. 1. Cross section of the full system model.

description given below. The diagonal lines show the kinematic direction of the thread bearing surfaces.

1) *Barrel assembly:* This model includes about 0.6 meter of the breech end of the barrel including the obturator pad seat, tube to ring threads and two pilot surfaces. A small portion at the forward end uses an increased mass to replace the unmodeled portion of the barrel assemble. To further enhance the model the nodes at the muzzle end are constrained to a constant axial displacement.
2) *Breech ring:* This model is an axisymmetric approximation of the breech ring with tube to ring threads, block to ring threads, mount to ring threads, the two pilot surfaces for the tube and a pilot surface for the mount. The outer surface contour is a rather unusual shape which resulted from a complicated development history and a need for a specific breech weight.
3) *Breech block:* This is a full model of the block including the block to ring threads on the outer diameter and the block-to-disk contact surface on the muzzle face.
4) *Obturator spindle:* This is a model of the spindle including the housing to spindle contact surfaces, the spindle to pad contact surface and the pad to disk contact. The small extension at the breech end retains the primer and is normally not on the centerline of the gun but has been moved in this model. The material stiffness for the lugs is reduced to model the fact that they are interrupted in the actual components.
5) *Obturator pad and rings:* The pad and rings are included as one body because sliding contact between them can be ignored. The fact that the pad is an elastomer and the rings are steel is modeled. Also since the rings are split rings the steel is given a very low hoop stiffness.
6) *Disc:* This is a simple washer located between the obturator pad and the breech block. It has a small sliding surface on each axial face.
7) *Mount:* The mount is modeled as a short cylinder with the ring-to-mount threads on the inside along with a mount-to-ring pilot surface. The outer volume uses the increased mass property to replace the mass of a facility mount.
8) *Cam Plate:* This is a non-structural plate which is bolted to the breech face of the block and is included because of it's inertial load on the block. The bolts are modeled using three simple springs which are preloaded by using a small interference of the contact surface with the block.
9) *Housing:* The housing model includes the mass of the firing mechanism, a contact surface at the muzzle end with the obturator spindle and the housing-to-spindle lug connection.

The dimensions for these components were taken directly from the Benét Laboratories drawings for the individual component and use the nominal dimensions for all of the gaps between contact surfaces.

Figure 2 is a detail of the housing and spindle showing how the housing is retained between the spindle body at the front (muzzle end) and a set of interrupted lugs at the breech end. With this system the assembly method is to insert the spindle into the housing, until it bottoms on the front interface and then a simple 1/4 turn locks in both the spindle and housing (using a spring pin). This requires a small gap or play between the two interfaces to allow easy assembly, which is a minimum of 0.000254 meter (0.010 inch) on the drawings. This fact will play a role in the conclusions of the analysis.

3. Contact surfaces

There are three types of interfaces in the overall model, small sliding contact, large sliding contact and

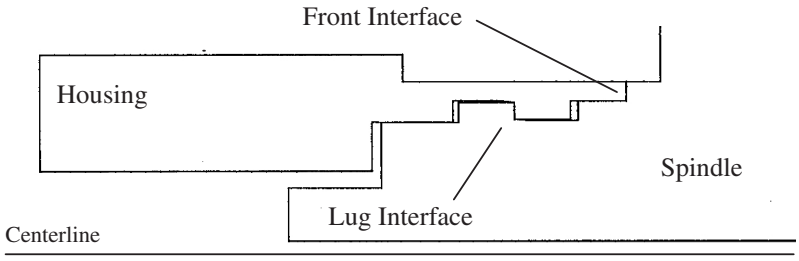

Fig. 2. Detail of the housing to spindle connection.

the complex thread interaction model. The small sliding surface formulation in ABAQUS (INTER3A) is used for the 3 pilot surfaces which close a radial gap and the five contacts surfaces which act in the axial direction and are all initially closed. The Slide Line (ISL22A) formulation for large sliding contact was used for obturator pad/spindle interaction and the obturator pad/barrel interaction. The pad is an elastomer which is subjected to very high loads and deformations. These deformations allow the pad/rings to have substantial motions relative to the barrel, breech block and spindle.

The three threaded connections are modeled using a combination of material replacement for threads and a set of oriented one-dimensional gap elements to provide the proper kinematics of the thread contact surfaces. This method has been used for several years [3] and was originally suggested by Bretel [4]. The first step is to calculate an equivalent orthotropic material with the same global stiffness as the full height of the threads. This material will occupy the space between the thread root and the pitch cylinder on each side of the connection. A detailed analysis of a single thread tooth was used to establish these properties using methods similar to work done in studies of thread performance [5–7]. The individual threads are then smeared into two rows of elements, with one row attached to each of the adjoining components. These rows meet at the pitch cylinder of the threads in a set of independent node pairs. The pairs are linked with 1-dimensional gap elements (GAPUNI), in a coordinate system which enables sliding parallel to the thread contact surface direction. The two connected points are at the same point in space and the direction vector for gap is defined normal to the thread contact surface. These two techniques model the stiffness and kinematics of the thread contact without resorting to defining individual thread teeth.

4. Loading

The primary loads are the pressure load in the chamber of the gun and the inertial loads from recoil. The pressure load covers the muzzle surface of the spindle, the bore surface (forward of the obturator pad) and the ID of the flame hole in the spindle. The pressure load is also reflected in a small concentrated load on the housing to simulate the axial load of the primer on the firing mechanism. The inertial loads are applied as a constant body force in the static solution and by using the free recoil condition for the dynamic solutions.

The three loads used reflect the behavior of M203 charge in an M199 Cannon. The basic pressure-time data in Fig. 3 was obtained from a XNOVAKTC [8–10] Interior Ballistic solution (IB) for this charge and was entered into ABAQUS as a table of 148 X-Y pairs. In this IB solution the projectile motion starts at 0.0048 seconds with the peak pressure of 310 mPa. is at 0.0099 seconds. Shot exit is at 0.020 seconds and the data table is cut off at 0.025 seconds. The peak pressure was used for the static solution along with a body force calculated from simple rigid body mechanics. The full pressure-time curve was used for the first dynamic solution to model the normal behavior of the breech. For the pressure spike case the time of the M203 charge was simply divided by 10 to produce a spike of the same pressure and shape but with a duration of 0.0025 seconds.

5. Results

The overall system model was debugged as a static problem and a test of the various contact surfaces. As always, in this sort of problem, most of the modifications made were in favor of a more realistic model, which generally makes the solution faster and more reliable. A case in point was that the disk was originally included as an extension on the block model, however

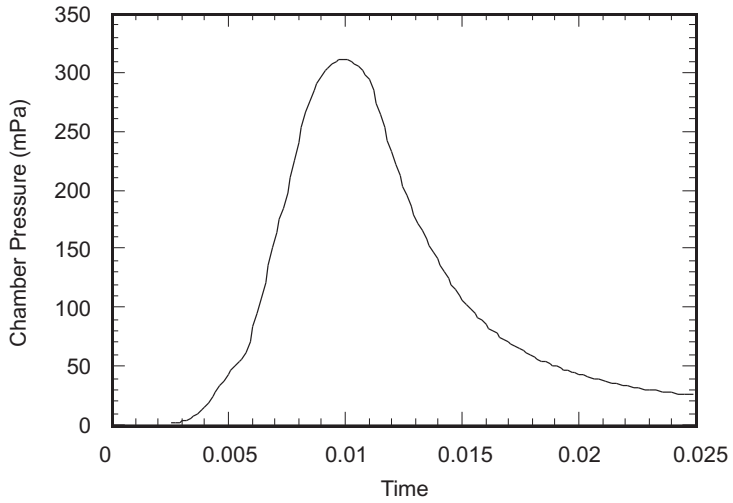

Fig. 3. P-T curve for the M203 charge.

this would not converge or would converge to an incorrect deformed shape. The disc is a bearing which operates to release the shear deformation between the block and the pad. Without fully modeling this function the 'hourglass' mode of the elements became a dominate behavior and produced a incorrect deformed shape. Inclusion of the disk as a separate component, with two contact surfaces, solved this problem.

The stress contour plot in Fig. 4 is typical of the general Mises stresses at the maximum pressure. Note the high stresses near the bore of the chamber, in the breech block and in the pad fillet of the spindle. Also note that there are no contours in the obturator pad which is in a state of hydro static compression. There is also a stress concentration in the ring at the thread relief for the block end threads. This rather mild stress concentration links with the stress concentration of the threads to produce the actual fatigue failure point in the ring.

After the static model was completed the dynamic solutions proceeded easily and the major problem became selecting and displaying the important results. An early decision was the selection of 4 points to use for stress comparisons of the various solutions. These points were all at high stress points of the major components. The first was at the bore of the barrel (3111-1), then one in the thread relief of the ring (6152-1), another in the block near the central hole (1166-7) and the last the pad fillet of the spindle (8201-1). Mises equivalent stresses for these four points and the three loading conditions are shown in Table 1. Note that there is no difference between the static solution and the standard M203 charge solution. The Pressure spike

Table 1
Mises Stress Comparison for three loading rates and four major components with stress in mPa. and a contour interval of about 68 mPa

Component	Static	M203 charge	Pressure spike
Tube			
3111	807.8	808.0	817.0
Ring			
6152	384.8	381.0	530.6
Block			
1166	999.8	993.6	1301.4
Spindle			
8208	883.2	878.0	1319.2

solution produces modest stress increases of as little as 1% for the bore of the tube to a high of 48% for the spindle. All of these were recorded at the time of maximum pressure in the chamber.

The spindle movement is a critical part of the operation of the obturator pad seal in this style of cannon. This is a Bridgeman unsupported area seal and uses the spindle to increase the pressure on the pad and force it against the pad seat of the barrel. The elastomer pad is compressed by the full axial pressure load on the spindle and is restrained on the pad seat and breech block . This seat is tapered so that as the pad moves rearward it must expand to meet the new diameter of the tube. At the same time the tube is expanding from the pressure load of the pad and the block is deflecting backward from the axial load on it. All of these combine to produce the spindle movement of 2.2 mm relative to either the block or the tube. This movement opens a large space between the spindle and the tube, which would allow the elastomer pad to extrude out if the split rings were not in place. The front split ring

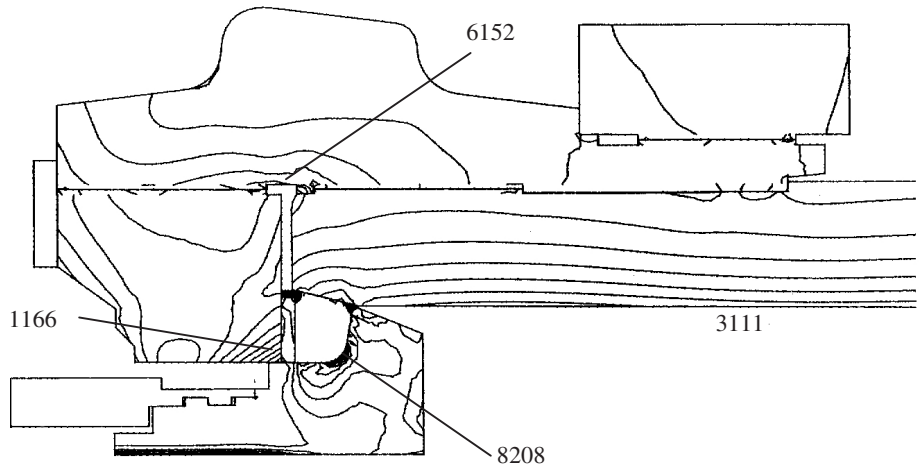

Fig. 4. Typical mises stress contour at a pressure of 310 mPa.

prevents this extrusion along with its mating split ring in the smaller space between the tube and the disc.

The first dynamic solution used the pressure-time data for the M203 charge and some of the basic structural information reported in Table 1. This was a free recoil case which yielded a rigid body displacement of 0.0075 meter at the time of peak pressure and 0.088 meter at shot exit. The corresponding recoil velocities were 3.98 and 9.92 meter/second. These numbers tended to reinforce the quality of the solution. However a major goal was to study the contact conditions on the lugs and the front contact surfaces of the housing. This was done by plotting the contact stress against time, as shown in Fig. 5. This plot shows a rather complex behavior which is influenced by local natural frequencies. The general stress level is low with a maximum of about 55 mPa on the lugs. The front contact surfaces is only activated twice between 0.004 and 0.007 seconds. Certainly one would not predict any sort of failure from this response.

The last solution, for the pressure spike, was generally similar to the other two cases with some increase in general stresses as noted in Table 1. This small increase is not the case for the lug contact stress in the spindle and housing. Here a plot of contact stresses vs. time for the lugs and the front contact surface reveal a very different picture of the stress levels and a clear behavior is demonstrated. The maximum contact stress on the lugs has become 1125 mPa and the front contact surface is very active. At this high loading rate the housing bounces across the gap impacting heavily on both surfaces. The maximum stress has increased by a factor of 20 and the contact stress is approaching the yield strength of the steel. Clearly one could predict a possible failure for this case.

6. Discussion

The three solutions in this report are for quite different time frames and show different data when viewed from different perspective. When the data is viewed from a general structural viewpoint some important effects can be demonstrated. An example of this is that static analysis may be a valid assumption for the design of large cannon components, if the analysis is for a normal well behaved charge. If the propellant does not burn smoothly and pressure spikes are generated some components may be subject to increased stress conditions. This is the case for the spindle fillet which shows a 48% gain in Mises stress. However when we look in detail at the spindle/housing interactions a rather different picture emerges. In the static case there is nothing of any interest the primer load pushes the housing against the spindle lug at an average of 11.4 mPa and nothing more. However when the normal pressure time curve is introduced a much more complex behavior is introduced and the contact load varies rapidly, at low stresses. Then at very high rate loads, another behavior is demonstrated in which the the housing bounces rapidly between the front contact surface and the lug surface resulting in high contact surfaces and possible failure of the lugs.

It is not enough to solve large complex finite element models of complicated structures and casually view the results. These models create enormous volumes of

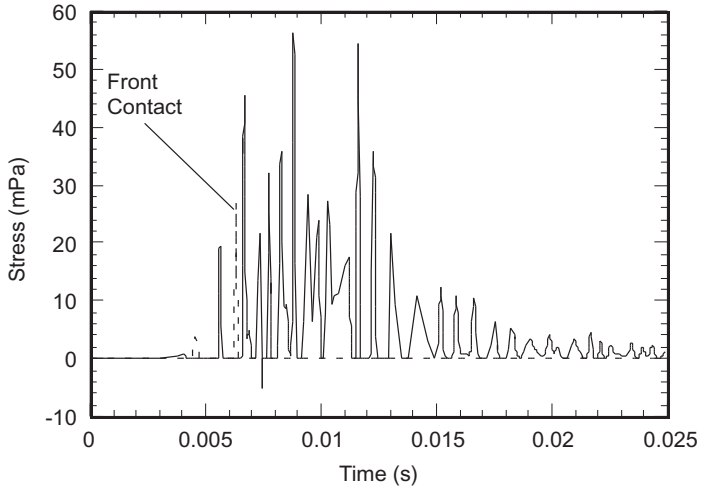

Fig. 5. Lug/front contact stress normal M203 charge.

information which must be critically evaluated to find the pertinent information. In this case the initial request was look at an explanation for the bearing failure of the spindle lugs which prompted the investigation of the lug contact stresses. The information on variation of general stresses with loading rate is one of the many other areas that may be investigated along with the primary analysis goal. Another point is the necessity of doing more than one analysis. The interesting part of this study is the comparison of three different loading rates and not the results of any single computer run. It should be pointed out that the results shown in this paper are for three runs using the same structural model, the same computer code (ABAQUS) and the same solution tolerance for the dynamic load cases.

This work demonstrates the old concept, that dynamic response is a function of structural stiffness and mass. The tube which is both massive and stiff, shows limited dynamic effects, while the block and spindle shows a substantial increase in stress as a result of the interaction with the rather soft pad. The ring shows some dynamic effect and is in the middle ground with good stiffness and mass. But the king of problems is involved the the housing which is not only the lightest component, but it interacts with a gap which has no stiffness at all. While the work may continue to make the solutions more efficient, this report provides a consistent set which can be used for comparisons.

7. Conclusion

This work tends to validate the very old idea that structural analysis of cannon breeches can be done by quasi-static methods. The burning of propellants is not an explosion, but a deflagration which should result in a rather smooth and (relatively) slow pressure time curve. However this is only true for the major structural components and a well behaved propellant charge. When high level pressure spikes are involved the stress picture changes and the changes can be rather dramatic.

Acknowledgement

The author wishes to acknowledge the support of Mr. Richard Hasenbein and Mr. Stephen VanDyke-Restifo of Benét Laboratories for support in this work. The author also wishes to thank Mr. George Pflegl for his advice and council.

References

[1] ABAQUS Theory Manual Version 5.7, Hibbitt, Karlsson & Sorenses, Inc., 1080 Main St., Pawtucket, RI, 1997.
[2] ABAQUS Users Manual Version 5.7, Hibbitt, Karlsson & Sorenses, Inc., 1080 Main St., Pawtucket, RI, 1997.
[3] G.P. O'Hara, *Analysis of a Large High Pressure Vessel Closure,* ASME Pressure Vessels & Piping Conference, Orlando FL, PVP Vol. July 1988 Also US Army Armament Research Development and Engineering Center (ARDEC), Technical Report, ARCCB-TR-89003, January 1989.
[4] J.L. Bretl, *Finite Element Analysis for General Solids and Threaded Connections,* University of Wisconsin-Madison, Ph.D. Thesis Applied Mechanics, 1978.
[5] G.P. O'Hara, Stress Concentrations in Screw Threads, Eighth NASTRAN Users' Colloquium, Goddard Space Flight Center, NASA Conference Publication 2131, October 1979, pp. 65-77. Also US Army Armament Research Development and Engineering Center (ARDEC), Technical Report, (with appendix) ARLCB-TR-80010, April 1980.

[6] G.P. O'Hara, Elastic-Plastic Comparison of Three Thread Forms, Proceedings of the Eighth US Army Symposium on Gun Dynamics, Newport, RI, May 1996, pp. 18-1–18-10.
[7] G.P. O'Hara and Elastic Comparison of Four Thread Forms, ASME Pressure Vessels & Piping Conference, PVP Vol. 344, Orlando, FL, July 1997.
[8] P.S. Gough, *The NOVA Code: A users Manual*, Indian Head Naval Ordnance Station, Contractor Report, IHCR-80-8, 1980.
[9] P.S. Gough, *The XNOVA: A Users Manual*, Indian Head Naval Ordnance Station, Contractor Report, N00174-86-M-4336, PGA 88-2, December 1987.
[10] P.S. Gough, The XNOVAKTC Code, US Army Ballistic Research Laboratory, Final Report, Contract DAAK11-85-D-00002, Task II, PGA-TR-86-1, March 1986.